



Evolutionary Characteristics of Concrete Damage in Poured-in-place Pile

Yangzi Liu*

School of urban and rural construction, Chengdu Agricultural College, Chengdu, Sichuan, 611130, China

* Corresponding author's e-mail address: 124190270@qq.com

Abstract. The application of concrete materials in poured-in-place pile engineering is extensive. Understanding the characteristics of concrete materials has a significant impact on the safe construction of poured-in-place piles. Therefore, this study investigates the evolutionary characteristics of concrete damage in poured-in-place piles using Acoustic Emission (AE) monitoring technology. The research findings reveal that concrete in poured-in-place piles mainly experiences brittle failure. The damage process can be divided into the stable deformation stage and the rapid crack propagation stage. Additionally, the point where $D=0.20$ is defined as the point of accelerated damage, while the point where $D=0.40$ is defined as the critical damage point. Furthermore, a fitting equation for the damage curve is obtained based on the exponential function, which can be used to predict the unstable failure of concrete materials in poured-in-place piles.

Keywords: Poured-in-place pile; Concrete; Damage; Acoustic Emission

1 INTRODUCTION

Concrete is a common building material that is widely used in construction and infrastructure projects. It is known for its strength, durability, and high compressive strength, making it suitable for constructing structural elements of buildings such as walls, columns, and beams. Additionally, concrete is frequently used in transportation projects such as roadways, bridges, and tunnels, as well as in water management, marine engineering, and energy projects. Concrete is also utilized in protective engineering projects such as slope protection, revetments, and dams, as well as for various decorative architectural elements like flooring and wall coatings. Consequently, the analysis of damage and fracture characteristics of concrete materials is an important research direction, with numerous scholars conducting extensive studies in this field.

With the rapid development of non-destructive testing technology, the method of using acoustic emission (AE) to investigate the mechanical properties of concrete materials has been widely applied. When exploring the acoustic emission characteristics of concrete materials, parameter analysis and frequency domain analysis methods

are commonly used^[1]. In investigating the damage evolution characteristics of concrete materials, many researchers^[2-6] have employed digital image correlation (DIC) technology and acoustic emission (AE) technology simultaneously to obtain real-time surface displacement fields of specimens and internal acoustic emission signals. Some scholars^[7, 8] have also explored the relationship between the mechanical parameters of concrete materials and AE parameters through mathematical models. In order to reduce experimental costs, some researchers^[9-11] have investigated the damage patterns of concrete materials solely through acoustic emission (AE) technology.

In conclusion, there are currently many research methods available to investigate the mechanical mechanisms of concrete materials. However, many experiments require high cost investments. Therefore, this paper conducted uniaxial compression experiments on concrete materials of cast-in-place piles and solely monitored them dynamically through an acoustic emission system. Based on the experimental results mentioned above, the paper aims to explore the damage evolution characteristics of cast-in-place pile concrete materials. By reducing the cost of experimental investments, this study provides accurate reference for the normal construction of upper works on cast-in-place piles and monitoring of cast-in-place pile damage.

2 EXPERIMENTAL OVERVIEW

2.1 Experimental Samples

The concrete specimens used in this study were obtained from cast-in-place piles in road and bridge engineering. The concrete grade of the sampled piles is C30 (underwater condition). The mixture composition of the concrete is as follows: cement : sand : aggregate : water : admixture : blended material = 1 : 2.12 : 3.05 : 0.50 : 0.01 : 0.21. The concrete specimens are standard cylindrical specimens specified by the International Society for Rock Mechanics. They have a height of 100mm and a diameter of 50mm. The height-to-diameter ratio is between 2.0 and 2.5, meeting the dimensional requirements. The length error of all specimens is less than 2mm. The unevenness after grinding both end faces is within $\pm 0.05\text{mm}$. The end faces are perpendicular to the axis, with a maximum deviation of not more than 0.25° . The basic physical parameters of the concrete specimens are shown in Table 1. The concrete specimens are shown in Figure 1.



Fig. 1. Concrete sample

Table 1. Physical Properties of Concrete Sample

Rock sample number	Weight (g)	Diameter (mm)	Height (mm)	Density (g/cm ³)
H-1	475.4	49.65	100.22	2.45

2.2 Experimental Equipment

The equipment used for the mechanical and acoustic emission experiments in this study are the SAM-2000 electro-hydraulic servo rock triaxial loading system and the PXDAQ24260B acoustic emission system. As shown in Figure 2.

**Fig. 2.** Experimental equipment

This experiment aims to investigate the damage evolution characteristics of concrete in bored piles. Firstly, the concrete specimens were subjected to conventional uniaxial compression tests using the SAM-2000 electro-hydraulic servo rock triaxial loading system. The specimen used for the uniaxial compression test is labeled as H-1. The loading method for this mechanical experiment is displacement control, with a loading rate of 0.05mm/min.

During the acoustic emission (AE) experiments, the PXDAQ24260B acoustic emission system was used for monitoring. To improve monitoring accuracy, four sensors were employed for the AE experiments (as shown in Figure 3 for the layout of AE experiment sensors). Through AE monitoring, it was determined that the maximum ambient noise level in the laboratory was 35 decibels (dB). Therefore, the AE monitoring threshold was set at 45 dB. The sampling rate was set at 1.25 million samples per second (1.25M). The waveform maximum duration was set at 100 milliseconds (ms). The peak definition time (PDT), high-definition time (HDT), and high-level time (HLT) were set at 50 microseconds (μ s), 100 μ s, and 300 μ s, respec-

tively. Furthermore, the reliability of the experimental method and parameter settings mentioned above has been confirmed.

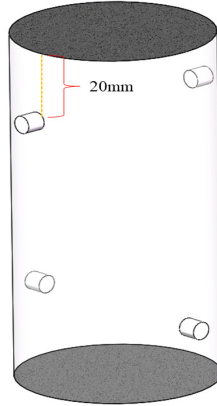


Fig. 3. Probe distribution scheme

3 PRECURSORY CHARACTERISTICS OF ACOUSTIC EMISSION (AE) PRIOR TO THE UNSTABLE FAILURE OF CONCRETE SAMPLE

Based on the above experiments, the stress-strain curve and evolution characteristics of AE ring counts of concrete specimens under uniaxial compression load were obtained. The specific results are shown in Figure 4.

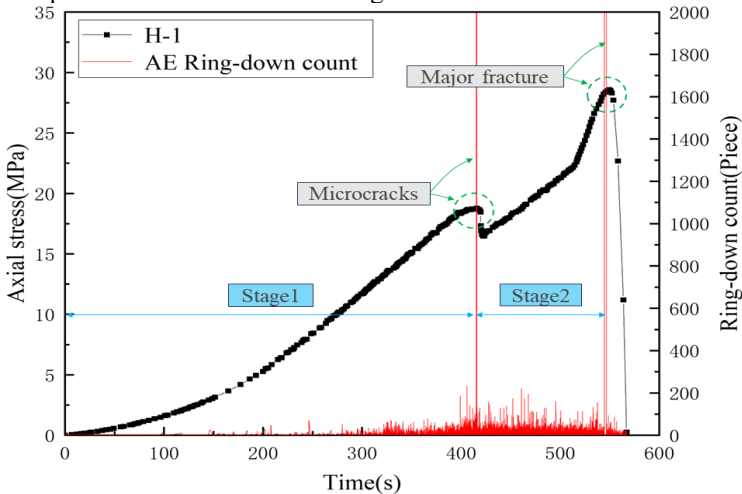


Fig. 4. Time-stress-ring-down count variation curve for sample H-1

From Figure 4, it can be observed that under uniaxial compression load, the concrete specimen primarily undergoes elastic deformation. Plastic deformation is not

significant. The specimen mainly undergoes brittle fracture when reaching the peak limit. During the elastic deformation stage, the stress curve is relatively smooth and the number of AE events is low. This indicates that during the elastic stage, the internal damage of the specimen is low, and there are not many microcracks generated. Near the point of unstable failure, the stress increases rapidly, and the number of AE events also increases rapidly. This indicates that at this point, the microcracks inside the specimen are rapidly propagating, causing accelerated fracture. Therefore, based on the development pattern of the stress curve and ring counts, the damage process of the specimen is divided into a stable deformation stage (Stage 1) and a rapid crack propagation stage (Stage 2).

At the beginning of Stage 2, the stress curve shows a significant decrease and there is a rapid increase in the number of AE events. This indicates the onset of microcracks. In Stage 2, the number of AE events remains relatively low. This phenomenon in Stage 2 is referred to as a calm period phenomenon, which is also the precursory AE characteristic of specimen failure. It can be seen that the damage and failure pattern of the specimen aligns perfectly with the development pattern of the ring counts. The macroscopic fracture characteristics of the concrete specimen are shown in Figure 5.



Fig. 5. Macroscopic fracture characteristics of concrete sample

4 EVOLUTION CHARACTERISTICS OF CONCRETE SAMPLE DAMAGE

The premise of conducting research on material damage evolution is the irreversibility of material damage. The extent of damage increases as cracks propagate. Therefore, the damage level of the material is represented by introducing damage variables. Different scholars have proposed different methods to define damage variables. For example, the ratio of damaged area to apparent area can be used as a damage variable, and the ratio of post-damage elastic modulus to initial elastic modulus can be used as a continuity factor. In recent years, with the technological innovations in industry, methods for defining damage variables using acoustic emission techniques and CT scanning techniques have gained widespread development.

This study utilizes acoustic emission techniques to indirectly define damage variables by obtaining corresponding variables. Firstly, it is assumed that the concrete material has no initial damage. When the concrete material is completely damaged, the cumulative ring count is denoted as F_{AE} . The cumulative ring count at any given time t is denoted as $F_{AE}(t)$. Therefore, the damage evolution equation of the concrete material can be represented as:

$$D = \frac{F_{AE}(t)}{F_{AE}} \tag{1}$$

The damage curve of the concrete specimen was obtained through the aforementioned calculation equation. The specific results are shown in Figure 6.

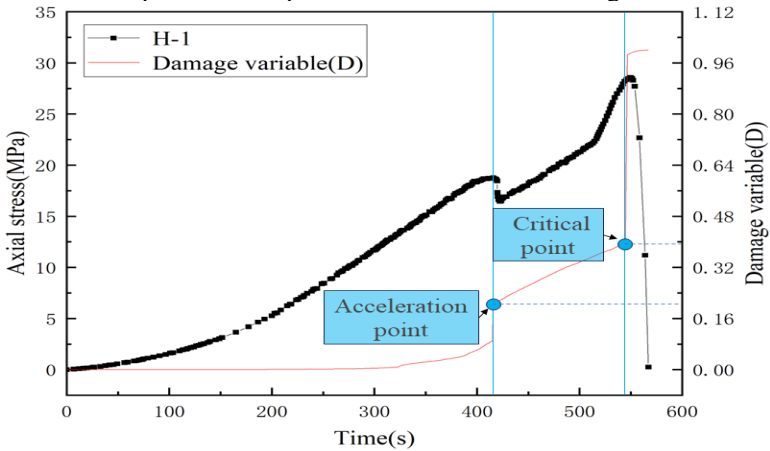


Fig. 6. Damage evolution characteristics of concrete sample

From Figure 6, it can be observed that the damage curve obtained through equation (1) fits well with the stress curve. This indicates that the calculation method using ring count as a variable is feasible. When $D \leq 0.20$, the damage curve is relatively smooth. However, when $D \geq 0.20$, the damage curve shows a significant acceleration in growth. Therefore, the point where $D = 0.20$ is defined as the damage acceleration point. This point is crucial in distinguishing between the stable deformation stage and the rapid crack propagation stage. When $D = 0.40$, the damage curve undergoes a sudden change and is very close to the peak point. Therefore, the point where $D = 0.40$ is defined as the damage critical point.

Based on the above results, it can be concluded that the evolution of the damage curve of the concrete specimen follows the trend of an exponential function. Therefore, the following exponential function is used for fitting.

$$y = y_0 + A1 * \exp((x - x_0) / t1) \tag{2}$$

The fitting results obtained through non-linear fitting using equation (2) are shown in Figure 7. The relationship is expressed by equation (3).

$$y = 0.04939 + 1.4974E-5 * \exp((x + 79.70988) / 58.59952) \tag{3}$$

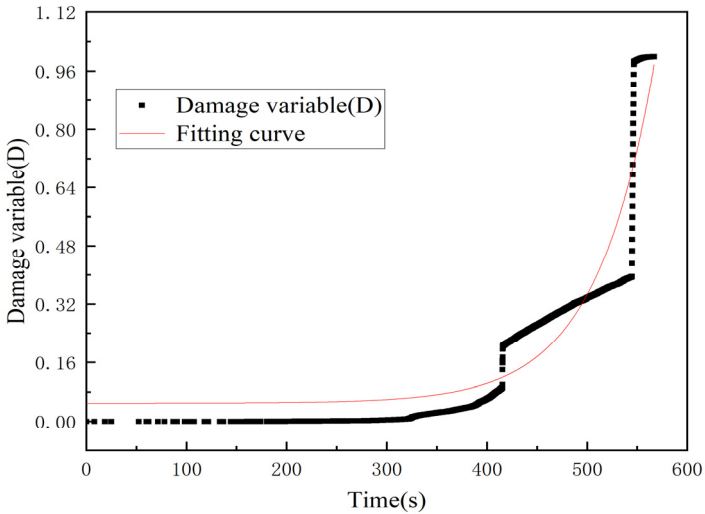


Fig. 7. Damage evolution characteristics of concrete sample

The coefficient of determination for the above fitting equation is 0.8042. Therefore, it is possible to predict the instability failure of cast-in-place pile concrete material using the above relationship. This is of significant importance for the safe development of engineering projects.

5 CONCLUSION

Based on the above analysis, it can be concluded that cast-in-place pile concrete primarily undergoes brittle failure when subjected to uniaxial loading. By combining Acoustic Emission (AE) monitoring technology with the development pattern of stress-strain curve and ringing count, the damage process of the specimen can be divided into two stages: stable deformation stage (Stage 1) and rapid crack propagation stage (Stage 2). The damage variable is defined using the ringing count, and the damage curve of the concrete specimen is obtained accordingly. Based on the development pattern of the damage curve, the point where $D = 0.20$ is defined as the damage acceleration point, and the point where $D = 0.40$ is defined as the damage critical point. Furthermore, an exponential function is used to fit the damage curve, and the coefficient of determination is 0.8042. This fitting equation can be used to predict the instability failure of cast-in-place pile concrete material. Therefore, during the construction of upper works on cast-in-place piles, it is possible to monitor the damage of cast-in-place piles in real-time based on the aforementioned results and using non-destructive testing equipment such as acoustic emission. This provides assurance for the safe construction of the entire project. In the future, based on the principles of acoustic emission localization, it will be possible to perform three-dimensional localization of the rupture points in cast-in-place piles. By com-

binning the research results of this paper, three-dimensional visualization and prediction of unstable failure in cast-in-place piles can be achieved.

Fund project: College-level project of Chengdu Agricultural College: Study on risk assessment and prevention of geological disasters in plateau area under the strategy of Rural Revitalization (22zr113)

REFERENCE

1. YU, A. P. CHEN, Z. H. ZHANG, L. LI, X. X. SHI, J. X. FU, F. (2023) Study on AE characteristics of concrete with different w/c ratio under uniaxial compression. *Structures*, 58.
2. DAI, S. H. LIU, X. L. NAWNIT, K. (2019) Experimental Study on the Fracture Process Zone Characteristics in Concrete Utilizing DIC and AE Methods. *Appl Sci-Basel*, 9(7).
3. MOROZOVA, N. SHIBANO, K. SHIMAMOTO, Y. SUZUKI, T. (2023) Influence of the Pre-Existing Defects on the Strain Distribution in Concrete Compression Stress Field by the AE and DICM Techniques. *Appl Sci-Basel*, 13(11).
4. MANUELLO, A. NICCOLINI, G. CARPINTERI, A. (2019) AE monitoring of a concrete arch road tunnel: Damage evolution and localization. *Eng Fract Mech*, 210: 279-87.
5. SHIMAMOTO, Y. TAYFUR, S. ALVER, N. SUZUKI, T. (2023) Identifying effective AE parameters for damage evaluation of concrete in headwork: a combined cluster and random forest analysis of acoustic emission data. *Paddy Water Environ*, 21(1): 15-29.
6. LI, G. D. GU, J. R. REN, Z. Y. ZHAO, F. N. ZHANG, Y. Q. (2021) Damage Evaluation of Concrete under Uniaxial Compression Based on the Stress Dependence of AE Elastic Wave Velocity Combined with DIC Technology. *Materials*, 14(20).
7. MA, G. F. DU, Q. J. (2020) Structural health evaluation of the prestressed concrete using advanced acoustic emission (AE) parameters. *Constr Build Mater*, 250.
8. ZHANG, X. C. SHAN, W. C. ZHANG, Z. W. LI, B. (2018) AE monitoring of reinforced concrete squat wall subjected to cyclic loading with information entropy-based analysis. *Eng Struct*, 165: 359-67.
9. LUO, T. PAN, X. F. TANG, L. Y. SUN, Q. PAN, J. J. (2022) Research on Splitting-Tensile Properties and Failure Mechanism of Steel-Fiber-Reinforced Concrete Based on DIC and AE Techniques. *Materials*, 15(20).
10. ZHANG, H. JI, S. S. WANG, L., JIN, C. J. LIU, X. Y. LI, X. C. (2022) Study on dynamic splitting tensile damage characteristics of basalt fiber reinforced concrete based on AE and DSCM. *J Build Eng*, 57.
11. GENG, J. S. SUN, Q. ZHANG, Y. C. CAO, L. W. ZHANG, W. Q. (2017) Studying the dynamic damage failure of concrete based on acoustic emission. *Constr Build Mater*, 149: 9-16.

Open Access This chapter is licensed under the terms of the Creative Commons Attribution-NonCommercial 4.0 International License (<http://creativecommons.org/licenses/by-nc/4.0/>), which permits any noncommercial use, sharing, adaptation, distribution and reproduction in any medium or format, as long as you give appropriate credit to the original author(s) and the source, provide a link to the Creative Commons license and indicate if changes were made.

The images or other third party material in this chapter are included in the chapter's Creative Commons license, unless indicated otherwise in a credit line to the material. If material is not included in the chapter's Creative Commons license and your intended use is not permitted by statutory regulation or exceeds the permitted use, you will need to obtain permission directly from the copyright holder.

